Accumulation and removal of Si impurities on β-Ga_2O_3 arising from ambient air exposure

Cite as: Appl. Phys. Lett. **124**, 111601 (2024); doi: 10.1063/5.0191280
Submitted: 12 December 2023 · Accepted: 25 February 2024 ·
Published Online: 11 March 2024

View Online

Export Citation

CrossMark

J. P. McCandless,[1,a] C. A. Gorsak,[2] V. Protasenko,[1] D. G. Schlom,[2,3,4] Michael O. Thompson,[2] H. G. Xing,[1,2,3] D. Jena,[1,2,3] and H. P. Nair[2]

AFFILIATIONS

[1]School of Electrical and Computer Engineering, Cornell University, Ithaca, New York 14853, USA
[2]Department of Materials Science and Engineering, Cornell University, Ithaca, New York 14853, USA
[3]Kavli Institute at Cornell for Nanoscale Science, Ithaca, New York 14853, USA
[4]Leibniz-Institut für Kristallzüchtung, Max-Born-Str. 2, Berlin, 12489, Germany

[a]Author to whom correspondence should be addressed: jmccandless@cornell.edu

ABSTRACT

Here, we report that a source of Si impurities commonly observed on (010) β-Ga_2O_3 is from exposure of the surface to air. Moreover, we find that a 15 min hydrofluoric acid (HF) (49%) treatment reduces the Si density by approximately 1 order of magnitude on (010) β-Ga_2O_3 surfaces. This reduction in Si is critical for the elimination of the often observed parasitic conducting channel, which negatively affects transport properties and lateral transistor performance. After the HF treatment, the sample must be immediately put under vacuum, for the Si fully returns within 10 min of additional air exposure. Finally, we demonstrate that performing a 30 min HF (49%) treatment on the substrate before growth has no deleterious effect on the structure or on the epitaxy surface after subsequent Ga_2O_3 growth.

Published under an exclusive license by AIP Publishing. https://doi.org/10.1063/5.0191280

12 March 2024 15:45:33

In recent years, there has been growing interest in the field of Ga_2O_3-based field-effect transistors (FETs). Ga_2O_3, particularly in the β-phase, has emerged as a very promising ultra-wide bandgap semiconductor with $E_g \sim 4.7$ eV.[1] This wide bandgap, along with the availability of large-area melt-grown substrates,[2] makes β-Ga_2O_3 an excellent candidate for high-voltage transistors for power applications.[3,4]

To achieve high-performance FETs, precise control of the doping density and of the spatial distribution of carriers is critical. In lateral devices, for example, a parallel conducting channel at the interface between the substrate and epitaxial layers can result in high reverse-bias leakage currents.[5] This is also a challenge for realizing high-electron mobility transistors (HEMTs). In HEMTs, the carrier mobility is enhanced through the creation of 2D electron gases.[6] By confining carriers within a well and spatially separating this well from the chemical doping sources, impurity scattering can be reduced leading to increased mobilities. Experimentally, however, the performance of β-Ga_2O_3 HEMTs has been limited due to large reverse leakage currents and reduced apparent mobilities, which have been attributed to the presence of a parallel conducting channel at the epitaxy-substrate interface.[5,7,8]

This parallel conducting channel is thought to be caused by the accumulation of Si impurities on Ga_2O_3 substrates.[9–12] This is a known issue in other compound semiconductors such as GaAs and GaN.[13–15] Consequently, it is imperative to investigate and understand the source, behavior, and removal of Si impurities to reduce their impact on the electrical performance of electron devices.

In an earlier work,[12] while addressing doping control in Si-doped β-Ga_2O_3 grown by molecular-beam epitaxy (MBE), it was discovered that a few unintentionally doped (UID) samples would show electrical conductivity, while others would not when measured by the Hall effect. A secondary-ion mass spectrometry (SIMS) profile of such a sample is shown in Fig. 1(a). The sample is a UID β-Ga_2O_3 film grown by MBE on a (010)-oriented edge-defined film-fed grown Fe-doped β-Ga_2O_3 substrate from Novel Crystal Technology (NCT).[2] At the epitaxy-substrate interface, there is a large Si peak (red trace) with a peak density of $\sim 2 \times 10^{19}/cm^3$. The average Fe density (blue trace) within the substrate is $\sim 7 \times 10^{17}/cm^3$. Despite being UID, with $N_d = 1.8 \times 10^{16}/cm^3$ in the epitaxial films, the sample displayed a free carrier sheet density of $2.2 \times 10^{13}/cm^2$ and a mobility of $\sim 10\ cm^2/V\,s$ when measured by the Hall effect.

A series of other similar samples were also measured by SIMS. Figure 1(b) shows the peak interface value of Si (red triangles) along with the average Fe value within the substrate (blue circles) for eight different samples. For these samples, the substrates were prepared with

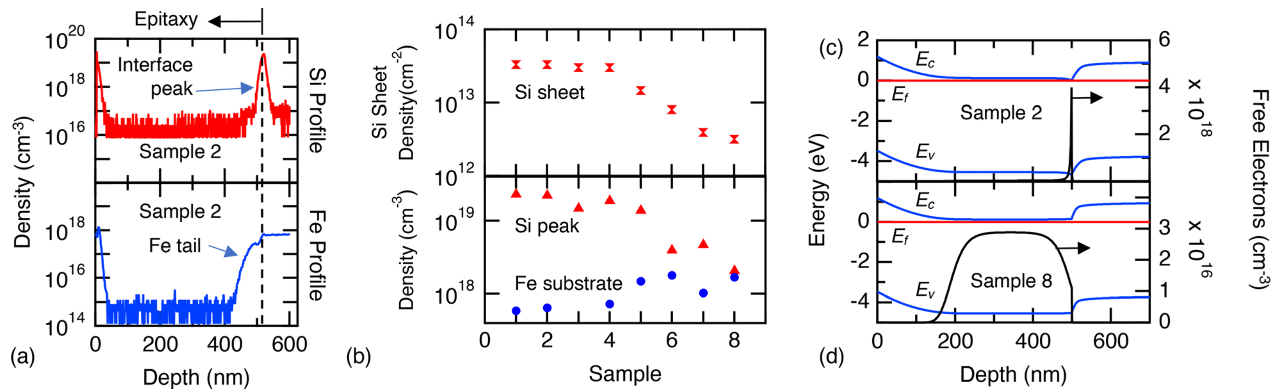

FIG. 1. (a) SIMS measurements of a UID-Ga_2O_3 sample with the Si peak at the epitaxy-substrate interface. The Fe is uniform within the substrate and then presents a tail into the film. (b) Eight samples, measured by SIMS, are shown with the average Fe density of the substrate in blue, and the interfacial Si peak value shown with red triangles. The Si interfacial peaks were integrated, and the values are shown as red hourglasses. For all samples shown, the substrate was prepared with a standard solvent clean only. (c) and (d) Calculated energy band diagrams with the epitaxy-substrate interface at 500 nm. (c) The energy band diagram for the case where the conduction band is pulled below the Fermi level at the epitaxy-substrate due to a large density of uncompensated Si dopants. Consequently, the free carriers are confined to the interface. (d) The calculated energy band diagram for a case where the interfacial charge from Si is fully compensated by the Fe within the Fe-Ga_2O_3 substrate. As a result, the conduction band is not pulled below the Fermi level, and the electron density is centered within the film.

solvent cleans only. The peak Si interface density was integrated, and the sheet densities are indicated with red hourglasses. There is significant variation in Si and Fe values among the samples.

To understand how the Fe and Si variations affect the energy band diagram, two cases were modeled with a 1D Poisson–Schrödinger self-consistent solver. The Si interface peak was simulated as a sheet charge, equal to the integrated interface peak value. Figure 1(c) shows the simulated energy band diagram for the case when there is a large difference between the Si peak density and the Fe substrate density ($N_d = 2.2 \times 10^{19}/\text{cm}^3$ and $N_a = 6.5 \times 10^{17}/\text{cm}^3$), similar to what is observed for sample 2 in Fig. 1(b). Due to the large uncompensated interfacial Si charge, the conduction band is pulled below the Fermi level. This results in a large density of free carriers confined to the interface ($n_s = 2.2 \times 10^{12}/\text{cm}^2$). Figure 1(d) shows the simulation for the case where the Si peak density and the Fe substrate density are of similar values ($N_d = 1.7 \times 10^{18}/\text{cm}^3$ and $N_a = 2.1 \times 10^{18}/\text{cm}^3$), like what is observed for sample 8 in Fig. 1(b). In this case, the conduction band does not go below the Fermi level, and the profile of the free carriers is centered within the epitaxial film with a sheet density of $n_s = 8.2 \times 10^{11}/\text{cm}^2$. Figure 1(d) is an example of the desired condition with no parallel conduction channel.

This Si and Fe variations and the corresponding variation in free carrier densities hinder the successful design and operation of FETs. To address this variation and the resulting uncompensated charges, we examined methods aimed at reducing or removing the Si from the interface. We found that exposing the sample surface to hydrofluoric acid (HF) (49%) for at least 15 min before growth reduced the Si density by $\sim$ 1 order of magnitude.

A quantitative study of the uncompensated charge is complicated due to the significant Si interfacial variability among substrates. To determine the efficacy of various surface treatments, it is essential to know the sheet density *a priori*. There are several possible sources of the Si contaminants, including adsorption of siloxanes from the air onto the Ga_2O_3 surface,[16] adsorption of Si onto the Ga_2O_3 surface from the colloidal silica slurry used for chemical-mechanical polishing of the substrates,[17,18] unintentional deposition from the quartz plasma bulb used in MBE systems, re-deposition from the walls of the metal-organic chemical vapor deposition (MOCVD) quartz chamber,[19,20] and desorption and re-deposition of Si from the growth chamber walls.[21,22]

To investigate the accumulation of Si from siloxanes in the air, MBE was used to grow UID-Ga_2O_3 on 1×1 cm^2 (010) Fe-Ga_2O_3 substrates from NCT. Before loading, the substrate was sonicated in acetone, IPA, and then DI water for 5 min each. A Ga flux of 1.1 nm^{-2} s^{-1}, O flux of 2.0 nm^{-2} s^{-1}, and plasma power of 250 W were used during the growth. The growth temperature, based on a thermocouple reading, was 770 °C. During the growths, the MBE chamber walls are kept cold by flowing liquid nitrogen through the chamber cryoshroud to prevent possible re-deposition of Si from the chamber walls onto the sample surface. After growing a $\sim$ 43 nm thick Ga_2O_3 layer, the sample was unloaded from the MBE and moved to a fume hood, where it was exposed to air for varying amounts of times, as specified in Fig. 2(a) above each peak. Then, the sample was reloaded in the MBE for the growth of another $\sim$ 43 nm Ga_2O_3 layer. In the middle of each Ga_2O_3 layer, a 4.5 nm $(Al, Ga)_2O_3$ (Al $\sim$ 8%) layer was grown as a marker for the SIMS measurements [see layer structure in Fig. 2(a), inset].

Figure 2(a) shows the Si contamination, measured by SIMS, as a function of the depth. The residence time of the sample in the fume hood between Ga_2O_3 layer growths is noted above each Si peak. At this time, it is unknown why the background Si density (mid-10^{17}/cm^3) is higher than what is observed in Fig. 1(a) ($2.27 \times 10^{16}/\text{cm}^3$). Figure 2(b) plots the sheet density obtained by integrating each peak in Fig. 2(a) as a function of the air exposure time, which ranged from 20 min to 18 h. Three different layers were exposed for 40 min, from which the standard error was calculated ($\pm 2.68 \times 10^{11}/\text{cm}^2$) and was used for generating the error bars; the error bars are obscured by the symbols on the plot. The Si sheet density saturates to $6.25 \times 10^{12}/\text{cm}^2$, reaching 90% after 4.75 h of air exposure. The data are fit by a Lagergren pseudo-first order kinetic equation

12 March 2024 15:45:33

Published under an exclusive license by AIP Publishing

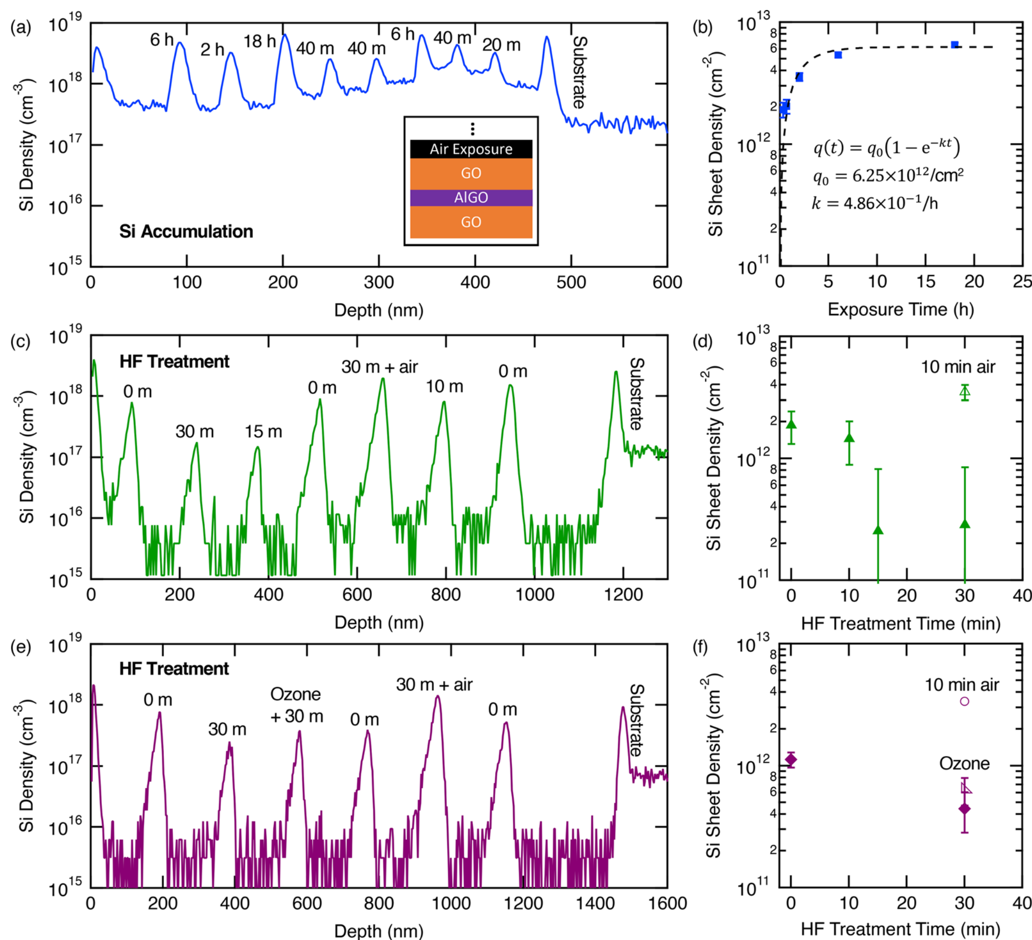

FIG. 2. (a) and (b) To study the accumulation of Si on Ga_2O_3 surfaces. (a) The Si profile obtained by SIMS for a UID-Ga_2O_3 sample grown by MBE. The substrate was prepared with the standard solvent clean only. Each peak corresponds to the amount of time the virgin Ga_2O_3 surface was exposed to air. In between each exposure, UID-Ga_2O_3 is grown. Exposure times ranged from 20 min to 18 h. Inset shows the repeating layer structure for each experiment. (b) The integrated sheet density obtained from panel (a) as a function of the exposure time. (c)-(f) To study the prospect of removing Si with HF from Ga_2O_3 surfaces grown by MOCVD. (c) For each layer, the virgin surface is exposed to air for 2 h, and then, the surface is treated in HF (49%) for the time specified above each peak. (d) The integrated peak density obtained in panel (c) as a function of HF exposure time. (e) The same process as described for (c) with the addition of a UV-ozone treatment step. Additionally, while the substrate shown in (c) was prepared with the standard solvent clean, the substrate shown in (e) was treated with solvents, HF (49%), piranha, UV-ozone cleaner, and HF again. (f) The integrated peak values from panel (e).

$q(t) = q_0(1 - e^{-kt})$, where $q_0 = 6.25 \times 10^{12}\ \mathrm{cm}^{-2}$ and the rate constant $k = 4.86 \times 10^{-1}\ \mathrm{h}^{-1}$.[23]

Next, we investigated the use of 49% hydrofluoric acid (HF) treatment as a possible method of reducing the Si surface contamination. For Figs. 2(c)–2(f), metalorganic chemical vapor deposition (MOCVD) was used instead of MBE. The motivation for using MOCVD is that the sample can be loaded, and the reactor pumped faster than in the MBE system; this minimizes the potential for additional Si accumulation during the loading process.

As before, $1 \times 1\ \mathrm{cm}^2$ substrates were solvent cleaned and then loaded into an Agnitron Agilis 100 MOCVD system. Triethylgallium (TEGa) and trimethylaluminum (TMAl) were used as gallium and aluminum precursors, respectively, and ultra-high purity molecular oxygen (99.994%) was used as the oxidant. Ultra-high purity Ar (99.999%) was further purified with point-of-use purifiers and was used as the carrier gas. The Ga_2O_3 layers were grown at a reactor pressure of 15 Torr, substrate temperature of 800 °C with a TEGa molar flow of 77 μmol/min, and a O_2/TEGa molar ratio of 580. In the middle of each Ga_2O_3 layer, a $(Al, Ga)_2O_3$ (Al $\sim$ 4%) marker layer was grown at 900 °C with a reactor pressure of 50 Torr with TEGa and TMAl molar flows of 77 μmol/min and 2.6 μmol/min, respectively.

After the growth of each layer, the sample was removed from the reactor and placed in a fume hood for 2 h, enabling Si to accumulate on the surface. Next, the sample was placed in HF (49%) for the time specified above the peaks in Fig. 1(c). Finally, the sample was placed back into the reactor for the next Ga_2O_3 layer growth. This process was repeated, with freshly poured HF for each HF treatment time.

Three layers were exposed to air for 2 h with no HF treatment and serve as the control samples [peaks labeled "0 m" in Fig. 2(c)]. From these three layers, the standard error was estimated to be

12 March 2024 15:45:33

Published under an exclusive license by AIP Publishing

$\pm 5.62 \times 10^{11}/\text{cm}^2$. The other layers were treated with HF (49%) between 10 and 30 min after exposure to air and the Si accumulated. The peaks in Fig. 2(c) were integrated, and the values are plotted as a function of HF exposure time in Fig. 2(d). It is inconclusive whether there was a reduction in the Si density after the 10 min HF treatment, but after 15 min, there is a significant reduction in the Si sheet density by more than 85%. There is no statistical difference between the 15 min and the 30 min HF treatment. The layer labeled "30 m + air" was, like the others, exposed to air within the fume hood for 2 h, treated with HF for 30 min, but then left in air again for 10 min. Within 10 min, the accumulated Si exceeded that of the control layer. Note that for all layers, there is an additional, unavoidable $\sim$5 min exposure to air, while the sample is transported from the fume hood to the reactor, loaded, and pumped down.

The last sample, for which the SIMS profile is shown in Fig. 2(e), was a repeat of the experiment in Fig. 2(c), with the following exceptions: (i) for the "30 m + air" experiment, after the 30 min HF treatment, the sample was left on a lab bench for 10 min instead of the fume hood; (ii) for the layer labeled "Ozone + 30 m," the sample was placed in a tabletop UV-ozone cleaner for 20 min after being exposed to air for 2 h. This was in an effort to further oxidize any Si on the surface before the 30 min HF treatment.

The results seen in Fig. 2(f) again show that the Si was removed with a 30 min HF treatment, and that the Si re-accumulated on the Ga_2O_3 surface after 10 min in the air. In this study, there was no clear benefit from performing an ozone treatment step. It is worth noting, however, that the sample was placed on a Si carrier wafer inside the UV-ozone cleaner, which may have affected the result.

Finally, for the sample shown in Fig. 2(e), the bare substrate was cleaned by solvents, treated in HF (49%) for 30 min, etched with piranha for 15 min, exposed to the table top UV-ozone cleaner for 20 min, and, finally, treated in HF again for 30 min before the growth. The sheet density of this substrate peak is $1.5 \times 10^{12}/\text{cm}^2$. While this is the *lowest* interfacial Si value observed in this study, it is premature to conclude whether this is due to the natural variation among the substrates, or if this reduction is, in fact, due to the surface treatment.

Based on the data reported here and until more statistical work can be performed, we suggest the following recommendations: samples should be treated in HF (49%) for at least 15 min and immediately loaded into the growth chamber. Alternatively, SIMS measurements can be performed to quantify Si and Fe densities to ensure there is no uncompensated charge. Finally, care should be taken when studying interfacial impurities and the potential removal of the Si, since it is critical to know the Si value *before* any treatment due to the significant surface variability.

To understand the impact of a 30 min HF treatment on subsequent epitaxial growth, β-Ga_2O_3 was grown on two substrates concurrently. Both substrates were first cleaned by solvents, and then one was treated in HF (49%) for 30 min, while the other one was not. The samples were then co-loaded, and $\sim$ 550 nm of β-Ga_2O_3 was grown by MOCVD. The growth conditions were the same as those described earlier except there was no $(Al,Ga)_2O_3$ layer, and a 100 nm low temperature Ga_2O_3 buffer layer was grown first at 600 °C after which the growth temperature was increased to 800 °C for the remainder of the growth.[9]

To assess the structural quality, rocking curve measurements of the 020 diffraction peak were measured [Fig. 3(b)]. The full-width at half max (FWHM) was 27 arcsec post-growth for the sample cleaned with solvent only, while the sample with the 30 min HF treatment in addition to the solvent clean had a FWHM of 30 arcsec. After growth, the rms surface roughness, measured by atomic force microscopy (AFM), revealed that the two samples have comparable roughnesses, 0.92 and 0.67 nm, for the solvent only and the solvent plus 30 min HF treatment, respectively, [Figs. 3(c) and 3(d)]. This indicates that a 30 min HF treatment did not negatively impact the resulting crystalline quality or the surface morphology.

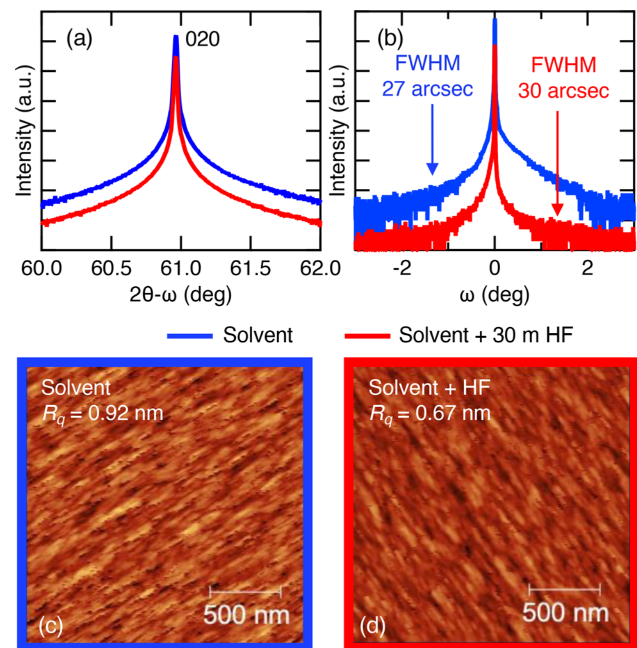

FIG. 3. The structural quality [(a) and (b)] and surface morphology [(c) and (d)] for two samples grown under the same conditions. One substrate was cleaned with solvents only (blue), and one substrate received a 30 min HF treatment after the solvents (red). The samples were co-loaded, and $\sim$ 550 nm of β-Ga_2O_3 was grown. (a) Coupled $2\theta - \omega$ measurements of the 020 Bragg peak were measured. (b) Rocking curves of the 020 Bragg peak show similar crystal qualities. The surface roughnesses of the samples reveled by AFM are similar (c) and (d).

In summary, our findings reveal substantial variation in Si and Fe concentrations within as-received (010) Fe-Ga_2O_3 substrates. This variation has important implications for the carrier compensation and, consequently, on the electrical properties and performance of devices fabricated on a given substrate. Our investigation indicates that ambient air is a significant source of Si contamination, and that treating the Ga_2O_3 surface with HF (49%) for a minimum of 15 min can reduce the Si impurity level by approximately one order of magnitude. While more experimentation is needed to determine the precise mechanism by which the HF treatment removes the Si from the surface, it is hypothesized here that the accumulated Si is oxidized by the ambient air and is subsequently removed with the HF treatment. To further reduce the potential for a parasitic conducting channel, compensation doping or *in situ* etching and removal of the interfacial Si will be required.

This research was supported by the Air Force Research Laboratory-Cornell Center for Epitaxial Solutions (ACCESS),

12 March 2024 15:45:33

Published under an exclusive license by AIP Publishing

monitored by Dr. Ali Sayir (No. FA9550-18-1-0529). JPM acknowledges the support of a National Science Foundation Graduate Research Fellowship under Grant No. DGE–2139899. CAG acknowledges support from the National Defense Science and Engineering Graduate (NDSEG) Fellowship. This work uses the CCMR and CESI Shared Facilities partly sponsored by the NSF MRSEC program (No. DMR-1719875) and MRI No. DMR-1338010, and the Kavli Institute at Cornell (KIC).

AUTHOR DECLARATIONS

Conflict of Interest

The authors have no conflicts to disclose.

Author Contributions

J. P. McCandless and C. A. Gorsak contributed equally to this paper.

J. P. McCandless: Conceptualization (lead); Data curation (lead); Formal analysis (lead); Investigation (lead); Methodology (lead); Visualization (lead); Writing – original draft (lead); Writing – review & editing (lead). **C. A. Gorsak:** Data curation (supporting); Formal analysis (equal); Investigation (equal); Methodology (equal); Visualization (supporting); Writing – original draft (supporting); Writing – review & editing (equal). **V. Protasenko:** Investigation (supporting); Resources (supporting). **D. G. Schlom:** Funding acquisition (supporting); Methodology (supporting); Resources (supporting); Writing – review & editing (equal). **M. O. Thompson:** Funding acquisition (supporting); Resources (supporting); Supervision (supporting); Writing – review & editing (equal). **H. G. Xing:** Funding acquisition (equal); Resources (equal). **D. Jena:** Data curation (supporting); Formal analysis (equal); Funding acquisition (lead); Resources (lead); Supervision (lead); Visualization (supporting); Writing – original draft (supporting); Writing – review & editing (equal). **H. P. Nair:** Formal analysis (supporting); Funding acquisition (equal); Investigation (supporting); Resources (lead); Supervision (lead); Writing – review & editing (equal).

DATA AVAILABILITY

The data that support the findings of this study are available from the corresponding author upon reasonable request.

REFERENCES

[1]H. H. Tippins, "Optical absorption and photoconductivity in the band edge of β-Ga_2O_3," Phys. Rev. **140**, A316–A319 (1965).
[2]A. Kuramata, K. Koshi, S. Watanabe, Y. Yamaoka, T. Masui, and S. Yamakoshi, "High-quality β-Ga_2O_3 single crystals grown by edge-defined film-fed growth," Jpn. J. Appl. Phys., Part 1 **55**, 1202A2 (2016).
[3]K. D. Chabak, N. Moser, A. J. Green, D. E. Walker, S. E. Tetlak, E. Heller, A. Crespo, R. Fitch, J. P. McCandless, K. Leedy, M. Baldini, G. Wagner, Z. Galazka, X. Li, and G. Jessen, "Enhancement-mode Ga_2O_3 wrap-gate fin field-effect transistors on native (100) β-Ga_2O_3 substrate with high breakdown voltage," Appl. Phys. Lett. **109**, 213501 (2016).
[4]K. D. Chabak, J. P. McCandless, N. A. Moser, A. J. Green, K. Mahalingam, A. Crespo, N. Hendricks, B. M. Howe, S. E. Tetlak, K. Leedy, R. C. Fitch, D. Wakimoto, K. Sasaki, A. Kuramata, and G. H. Jessen, "Recessed-gate enhancement-mode β-Ga_2O_3 MOSFETs," IEEE Electron Device Lett. **39**, 67–70 (2018).
[5]M. H. Wong, K. Sasaki, A. Kuramata, S. Yamakoshi, and M. Higashiwaki, "Electron channel mobility in silicon-doped Ga_2O_3 MOSFETs with a resistive buffer layer," Jpn. J. Appl. Phys., Part 1 **55**, 1202B9 (2016).
[6]R. Dingle, H. Störmer, A. C. Gossard, and W. Wiegmann, "Electron mobilities in modulation-doped semiconductor heterojunction superlattices," Appl. Phys. Lett. **33**, 665–667 (1978).
[7]E. Ahmadi, O. S. Koksaldi, X. Zheng, T. Mates, Y. Oshima, U. K. Mishra, and J. S. Speck, "Demonstration of β-$(Al_xGa_{1-x})_2O_3$/β-Ga_2O_3 modulation doped field-effect transistors with Ge as dopant grown via plasma-assisted molecular beam epitaxy," Appl. Phys. Express **10**, 071101 (2017).
[8]N. K. Kalarickal, Z. Xia, J. F. McGlone, Y. Liu, W. Moore, A. R. Arehart, S. A. Ringel, and S. Rajan, "High electron density $\beta-(Al_{0.17}Ga_{0.83})_2O_3/Ga_2O_3$ modulation doping using an ultra-thin (1 nm) spacer layer," J. Appl. Phys. **127**, 215706 (2020).
[9]A. Bhattacharyya, C. Peterson, T. Itoh, S. Roy, J. Cooke, S. Rebollo, P. Ranga, B. Sensale-Rodriguez, and S. Krishnamoorthy, "Enhancing the electron mobility in Si-doped (010) β-Ga_2O_3 films with low-temperature buffer layers," APL Mater. **11**(2), 021110 (2023).
[10]K. Azizie, F. V. E. Hensling, C. A. Gorsak, Y. Kim, D. M. Dryden, M. K. I. Senevirathna, S. Coye, S.-L. Shang, J. Steele, P. Vogt, N. A. Parker, Y. A. Birkhölzer, J. P. McCandless, D. Jena, H. G. Xing, Z.-K. Liu, M. D. Williams, A. J. Green, K. Chabak, A. T. Neal, S. Mou, M. O. Thompson, H. P. Nair, and D. G. Schlom, "Silicon-doped β-Ga_2O_3 films grown at 1 μm/h by suboxide molecular-beam epitaxy," APL Mater. **11**(4), 041102 (2023).
[11]P. Vogt, F. V. E. Hensling, K. Azizie, C. S. Chang, D. Turner, J. Park, J. P. McCandless, H. Paik, B. J. Bocklund, G. Hoffman, O. Bierwagen, D. Jena, H. G. Xing, S. Mou, D. A. Muller, S.-L. Shang, Z.-K. Liu, and D. G. Schlom, "Adsorption-controlled growth of Ga_2O_3 by suboxide molecular-beam epitaxy," APL Mater. **9**, 031101 (2021).
[12]J. P. McCandless, V. Protasenko, B. W. Morell, E. Steinbrunner, A. T. Neal, N. Tanen, Y. Cho, T. J. Asel, S. Mou, P. Vogt, H. G. Xing, and D. Jena, "Controlled Si doping of β-Ga_2O_3 by molecular beam epitaxy," Appl. Phys. Lett. **121**(7), 072108 (2022).
[13]K. Fu, H. Fu, X. Deng, P. Y. Su, H. Liu, K. Hatch, C. Y. Cheng, D. Messina, R. V. Meidanshahi, P. Peri, C. Yang, T. H. Yang, J. Montes, J. Zhou, X. Qi, S. M. Goodnick, F. A. Ponce, D. J. Smith, R. Nemanich, and Y. Zhao, "The impact of interfacial Si contamination on GaN-on-GaN regrowth for high power vertical devices," Appl. Phys. Lett. **118**, 22104 (2021).
[14]K. D. Choquette, M. Hong, H. S. Luftman, S. N. Chu, J. P. Mannaerts, R. C. Wetzel, and R. S. Freund, "GaAs surface reconstruction obtained using a dry process," J. Appl. Phys. **73**, 2035–2037 (1993).
[15]Y. Cao, T. Zimmermann, H. Xing, and D. Jena, "Polarization-engineered removal of buffer leakage for GaN transistors," Appl. Phys. Lett. **96**, 042102 (2010).
[16]H. C. Shields, D. M. Fleischer, and C. J. Weschler, "Comparisons among VOCs measured in three types of U.S. commercial buildings with different occupant densities," Indoor Air **6**, 2–17 (1996).
[17]M. E. Liao, K. Huynh, L. Matto, D. P. Luccioni, and M. S. Goorsky, "Optimization of chemical mechanical polishing of (010) β-Ga_2O_3," J. Vac. Sci. Technol. A **41**, 013205 (2023).
[18]J. P. Liu, J. H. Ryou, D. Yoo, Y. Zhang, J. Limb, C. A. Horne, S. C. Shen, R. D. Dupuis, A. D. Hanser, E. A. Preble, and K. R. Evans, "III-nitride heterostructure field-effect transistors grown on semi-insulating GaN substrate without regrowth interface charge," Appl. Phys. Lett. **92**, 133513 (2008).
[19]T. J. Asel, E. Steinbrunner, J. Hendricks, A. T. Neal, and S. Mou, "Reduction of unintentional Si doping in β-Ga_2O_3 grown via plasma-assisted molecular beam epitaxy," J. Vac. Sci. Technol. A **38**, 043403 (2020).
[20]K. Ikenaga, N. Tanaka, T. Nishimura, H. Iino, K. Goto, M. Ishikawa, H. Machida, T. Ueno, and Y. Kumagai, "Effect of high temperature homoepitaxial growth of β-Ga_2O_3 by hot-wall metalorganic vapor phase epitaxy," J. Cryst. Growth **582**, 126520 (2022).
[21]E. Welser, W. Guter, A. Wekkeli, and F. Dimroth, "Memory effect of Ge in III-V semiconductors," J. Cryst. Growth **310**, 4799–4802 (2008).
[22]F. Alema, G. Seryogin, A. Osinsky, and A. Osinsky, "Ge doping of β-Ga_2O_3 by MOCVD," APL Mater. **9**, 091102 (2021).
[23]S. Lagergren, "Zur theorie der sogenannten adsorption gelöster Stoffe," K. Sven. Vetenskapsakad. **24**, 1–39 (1898).

12 March 2024 15:45:33

Published under an exclusive license by AIP Publishing